Cell Calcium (2008) 44, 243–258

journal homepage: www.elsevier.com/locate/ceca

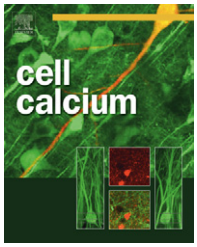

The cellular concentration of Bcl-2 determines its pro- or anti-apoptotic effect

C. Jane Hanson[a], Martin D. Bootman[a,*], Clark W. Distelhorst[b], Tullia Maraldi[c], H. Llewelyn Roderick[a,d]

[a] *Laboratory of Molecular Signalling, Babraham Institute, Babraham, Cambridge CB2 4AT, UK*
[b] *Departments of Medicine and Pharmacology, Comprehensive Cancer Center, Case Western Reserve University and University Hospitals of Cleveland, Cleveland, OH 44106, USA*
[c] *Department of Biochemistry ''G. Moruzzi'', University of Bologna, Via Irnerio 48, 40126 Bologna, Italy*
[d] *Department of Pharmacology, University of Cambridge, Tennis Court Road, Cambridge CB2 1PD, UK*

Received 5 April 2007; received in revised form 1 October 2007; accepted 17 November 2007
Available online 22 January 2008

KEYWORDS
Calcium;
Apoptosis;
Bcl-2;
Mitochondria

Summary Bcl-2 is an oncoprotein that is widely known to promote cell survival by inhibiting apoptosis. We explored the consequences of different expression paradigms on the cellular action of Bcl-2. Using either transient or stable transfection combined with doxycycline-inducible expression, we titrated the cellular concentration of Bcl-2. With each expression paradigm Bcl-2 was correctly targeted to the endoplasmic reticulum and mitochondria. However, with protocols that generated the greatest cellular concentrations of Bcl-2 the structure of these organelles was dramatically altered. The endoplasmic reticulum appeared to be substantially fragmented, whilst mitochondria coalesced into dense perinuclear structures. Under these conditions of high Bcl-2 expression, cells were not protected from pro-apoptotic stimuli. Rather Bcl-2 itself caused a significant amount of spontaneous cell death, and sensitised the cells to apoptotic agents such as staurosporine or ceramide. We observed a direct correlation between Bcl-2 concentration and spontaneous apoptosis. Expression of calbindin, a calcium buffering protein, or an enzyme that inhibited inositol 1,4,5-trisphosphate-mediated calcium release, significantly reduced cell death caused by Bcl-2 expression. We further observed that high levels of Bcl-2 expression caused lipid peroxidation and that the deleterious effects of Bcl-2 could be abrogated by the reactive oxygen species (ROS) scavenger Trolox. When stably expressed at low levels, Bcl-2 did not corrupt organelle structure or trigger spontaneous apoptosis. Rather, it protected cells from pro-apoptotic stimuli. These data reveal that high cellular concentrations of Bcl-2 lead to a calcium- and ROS-dependent induction of death. Selection of the appropriate expression paradigm is therefore crucial when investigating the biological role of Bcl-2.
© 2007 Elsevier Ltd. All rights reserved.

* Corresponding author. Tel.: +44 1223 496443; fax: +44 1223 496033.
E-mail address: martin.bootman@bbsrc.ac.uk (M.D. Bootman).

0143-4160/$ – see front matter © 2007 Elsevier Ltd. All rights reserved.
doi:10.1016/j.ceca.2007.11.014

1. Introduction

Bcl-2 is a well-known anti-apoptotic protein [1]. The identity and function of Bcl-2 were determined from a human B-cell lymphoma that had undergone a chromosomal translocation, which placed the Bcl-2 gene downstream of the IgH heavy chain enhancer [2]. The resultant increase in Bcl-2 expression gave the cells a profound survival advantage [3]. Bcl-2 is a 26 kDa protein that post-translationally inserts into cellular membranes via its c-terminal tail, with the amino-terminal bulk of the protein facing the cytosol. It has been shown to be present on the endoplasmic reticulum (ER), nuclear envelope and mitochondria [4]; the major sites of calcium (Ca^{2+}) flux within cells.

Ca^{2+} controls numerous cellular activities [5]. In particular, it is established that Ca^{2+} can promote apoptosis. Gross Ca^{2+} signals have been monitored in cells exposed to various pro-apoptotic stimuli [6,7], and buffering cellular Ca^{2+} can delay, or sometimes inhibit, cell death [7]. Recent studies have identified a number of ways in which cells' Ca^{2+} signalling systems can be modulated to either inhibit or promote apoptosis. It appears that many of the processes involved in storage, homeostasis or liberation of Ca^{2+} are targets of various components of the apoptotic machinery [8]. Of particular relevance to the present study, the release of Ca^{2+} from intracellular stores appears to be a key regulatory step [9]. Indeed, Bcl-2, and some of its homologues, have been demonstrated to modulate the mobilisation of the ER Ca^{2+} pool [10—13]. Somehow Bcl-2 prevents Ca^{2+} increases, or reduces the magnitude of Ca^{2+} transients so that cells can tolerate toxic death-inducing insults and survive until Ca^{2+} homeostasis has been re-established [7].

There have been many studies examining the consequence of Bcl-2 expression on ER Ca^{2+} homeostasis [8]. Several of these investigations have observed significant changes in ER Ca^{2+} content, but the direction of the effect (i.e. increase or decrease) has been curiously inconsistent [14]. Other studies have proposed that Bcl-2 regulates cellular Ca^{2+} signals via interaction with Ca^{2+} release channels [10,15], Ca^{2+} pumps [16], Ca^{2+} leak pathways [17] or mitochondria [18]. As pointed out recently [8], these mechanisms are not necessarily mutually exclusive. However, whether all of these mechanisms are all physiologically valid and equally significant is presently controversial. Some of these controversies may however be due to the cellular context; for example the cell type and the $InsP_3R$ isoforms expressed. Clearly, more work is required to establish the bona fide interaction between Bcl-2 and cellular Ca^{2+} signalling machinery.

The bulk of studies examining the impact of Bcl-2 on cellular Ca^{2+} signalling have employed heterologous expression of the gene encoding Bcl-2 under the control of a strong constitutively-active promoter. Both transient and stably transfected Bcl-2-expressing cells have been used. Each of these approaches has merits and drawbacks. Transient transfection is probably the most common method of over-expressing proteins. Gene expression is short-term as the heterologously introduced DNA is not integrated into the host genome. This approach allows for rapid over-expression of proteins of interest, without adaptation of the cell. However, very high average levels of expression can occur (>5—10-fold), albeit with considerable cell-to-cell variability, and transfection efficiency is unpredictable. With stable over-expression, the gene of interest is integrated into the host genome, thereby offering long-term selectable expression across an entire cell population. However, this experimental model takes time to set up, the site of integration into the genome cannot be controlled and adaptation can occur in cells in response to the stably over-expressed protein.

In our attempts to develop an experimental model to examine the role of Bcl-2 on Ca^{2+} signalling, we have examined the cellular consequences of transient and stable Bcl-2 expression. Our aim was to produce a model with the following characteristics: the sub-cellular localisation should be similar to that of native Bcl-2, over-expressed Bcl-2 should function in an anti-apoptotic manner, levels of expression should not be too high (<5-fold higher than endogenous), and furthermore, endogenous levels of Bcl-2 in the cell line used should be low so that the effects of expression of Bcl-2 and its mutants can be directly monitored. During the course of this work, we observed that the experimental paradigm used to modulate Bcl-2 expression had dramatic consequences for the cells. Rather than being pro-survival, when expressed at a high level, it was deleterious to the cell, inducing apoptosis as well as sensitising the cells to pro-apoptotic agents.

2. Materials and methods

2.1. Cell lines and reagents

Human Embryonic Kidney 293 cells (HEK-293) were obtained from Microbix (Ontario, Canada). The cells were obtained at passage 31, and used for no more than 15 further passages before being revived. Tetracyline-Regulated Expression 293 cells (T-REx-293), which are HEK-293 cells stably expressing the tetracycline repressor, were obtained from Invitrogen. Expression of the tetracycline repressor in TREx-293 cells allows for repression and de-repression of a modified CMV promoter containing Tet operator sequences. This enables regulation of genes contained within a pcDNA4/TO (Invitrogen) expression vector [19]. Ceramide was obtained from Sigma, staurosporine from Calbiochem, fura2 from Invitrogen and anti-malondialdehye (MDA) antibodies were from AbCam.

2.2. Expression plasmids

pEGFP-C1 was obtained from Clontech. The expression vector for GFP-tagged wild type human Bcl-2 (pGFP-Bcl-2) has been previously described [4]. To create the inducible GFP-Bcl-2 expression vector (pcDNA4/TO-GFP-Bcl-2) (TO-GFP-Bcl-2) the BglII/EcoR1 DNA fragment containing the cDNA encoding Bcl-2 was excised from pGFP-Bcl-2 and subcloned by ligation into BamH1/EcoR1-digested pcDNA4/TO-GFP. pcDNA4/TO-GFP was created by subcloning the Eco47III/Dra1 DNA fragment containing the cDNA encoding GFP and the multiple cloning sequence from pEGFP-C1 into similarly digested pcDNA4/TO. mRFP-calbindin was generated by subcloning a cDNA fragment encoding rat calbindin

(kind gift of B. Schwaller) at the 3′ end of mRFP (kind gift of R. Tsien). Specifically, mRFP was amplified by PCR using primers to append Nhe1 and HindIII restriction sites to its 5′ end 3′ end, respectively. Subsequent to digestion, this PCR product was ligated into a similarly digested pEGFP-C1 (Clontech), creating pmRFP-C1. To insert calbindin into this vector, it was first PCR-amplified using primers to append a HindIII restriction site to its 5′ end and a BamHI restriction site to its 3′ end. Following restriction digest this construct was ligated into a similarly digested pmRFP-C1.

2.3. Transient transfection

Cells were transfected at ∼75% confluency, 16 h prior to experimentation, using GeneJuice transfection reagent (Novagen), JetPEI transfection reagent (Q-BIOgene) or Lipofectamine 2000 (Invitrogen) according to the manufacturers' protocols. For imaging and flow cytometry, cells were transfected using GeneJuice or JetPEI, but for experiments where greater than 90% transfection was required, Lipofectamine 2000 was used.

2.4. Stable transfection

HEK-293 cells stably expressing GFP or GFP-Bcl-2 were generated by initial transient transfection, as above, followed by selection for expressing cells and maintenance in media containing 700 μg/ml G418. To ensure that the whole population was expressing the constructs following selection, cells were sorted based on their GFP fluorescence using a FACSDiVA cell sorter. Note that individual clones were not isolated. Rather the entire transfected population was selected and maintained.

2.5. Confocal imaging

To visualise the endoplasmic reticulum, cells were loaded with 500 nM ER-Tracker Blue-White DPX (Invitrogen) for 20 min in HBSS at 37 °C, then washed twice in HBSS and mounted in an imaging chamber. The imaging chamber was then placed in a heated stage-plate, which was maintained at 37 °C. To visualise mitochondria, cells were loaded whilst on the microscope stage with 250 nM tetramethylrhodamine ethyl ester (TMRE), a potentiometric mitochondrial dye (Invitrogen). Images of live cells were captured using a Zeiss LSM 510 META point-scanning confocal microscope, with a C-apochromat 63×, 1.2 numerical aperture water objective, and a pinhole set to 1 Airy unit for the red channel and corresponding pinholes set to give the same optical slice depth (0.7 μm) for all other channels. Using transmitted light, a differential interference contrast (DIC) image was taken simultaneously. GFP was excited at 488 nm using a multi-line argon laser, and the emission was collected using a 505—550 nm band pass filter. ER-tracker Blue-White DPX was excited at 405 nm using a blue diode laser and emission was collected using a 420—480 nm band pass filter. TMRE was excited at 561 nm using a red HeNe laser and emission was collected using the Zeiss Meta spectral detector between 603 and 688 nm.

2.6. Flow cytometry

In order to determine the level of GFP fluorescence, cells were analysed using a Becton Dickinson FACSCalibur. GFP was excited at 488 nm and emission was collected using a 530/30 nm band pass filter. To determine the proportion of cells with sub-G1 DNA content, cells were trypsinised to detach them from their plastic culture flasks, and then resuspended in the original media in which they were grown (to retain any apoptotic cells that were already detached). The cells were then washed twice in PBS and fixed in 70% ethanol/30% PBS at 4 °C overnight. Fixed cells were washed twice in PBS and resuspended at 10×10^6 cells/ml. They were then passed through a 25-gauge needle and treated with 25 μg/ml RNAse for 10 min. The cells were then stained with 0.5 mg/ml PI in the presence of 0.6% IGEPAL-630 for 2 h on ice. Cells were analysed for GFP and PI fluorescence using a Becton Dickinson FACSCalibur using excitation at 488 nm. GFP fluorescence emission was collected using a 530/30 nm band pass filter, and PI fluorescence using a 670 nm long pass filter.

2.7. Immunoblotting

Immunoblotting was used to detect expression levels of Bcl-2, $InsP_3R$ isoforms and cleavage of caspase-3. Lysates were prepared as previously described [20], though as many of the cells used in these experiments were apoptotic, both cells in the growth media and those that remained attached were pooled. To this end, cells were scraped into the overlying media prior to washing. 20 μg of protein lysates were resolved on 1 mm thick self-poured polyacrylamide gels. GFP-Bcl-2 and caspase-3 were resolved on 14 and 16% gels, respectively and transferred to nitrocellulose. GFP-Bcl-2 was detected using a monoclonal anti-Bcl-2 antibody (dilution 1:200, Santa Cruz) and caspase-3 was probed for using a polyclonal anti-caspase-3 antibody (dilution 1:250, Cell Signalling Technology). Enhanced chemiluminescence (ECL, Pierce) (for Bcl-2) or ECL Plus (Amersham) (for caspase-3) were used to detect immunoreactive bands after incubation with secondary antibodies conjugated to horseradish peroxidase (HRP) (dilution 1:10000, Jackson ImmunoResearch,). To determine band intensity, films were digitised using a Microtek ScanMaker i900 scanner, then images were black-white inverted and signals corresponding to immunoreactive bands were quantitated using ImageJ software (http://rsb.info.nih.gov/ij/).

2.8. Fura-2 imaging of transfected cells

Videoimaging of Fura-2-loaded cells was performed as previously described using a Sutter (Lambda Technologies, Brattleboro) filter wheel-based imaging system [21].

2.9. Immunofluorescence

MDA was detected by immunofluorescent staining of cells that had either been transfected with Bcl-2 (16 h post-transfection) or that had been exposed to ionomycin (10 μM; 2 h). To this end, cells were fixed and processed for

immunofluorescence as described previously [20]. MDA was detected using a rabbit polyclonal antibody diluted 1:50 in PBS containing 0.1% TRITON X-100 and 5% goat serum. Antibody staining was visualised using an anti-rabbit ALEXA-568 conjugated secondary antibody (dilution 1:500). Images were captured using a Zeiss LSM 510 META confocal microscope using a plan apochromat 60×, 1.40 n.a. oil immersion objective.

3. Results

3.1. Localisation and expression of transiently over-expressed GFP-Bcl-2

To examine the localisation of heterologously expressed Bcl-2, we employed a GFP-tagged form of wild-type Bcl-2 (GFP-Bcl-2) [4]. GFP was appended to the NH_2-terminus of Bcl-2, so as not to disrupt its COOH-terminal membrane targeting sequence. Confocal imaging of live HEK-293 cells 16 h post-transfection revealed that GFP-Bcl-2 co-localised with both the ER and mitochondria, thereby demonstrating the correct sub-cellular targeting of the fusion protein (Fig. 1A). Over-expression of GFP-Bcl-2 was confirmed by immunoblotting of total cell lysates, with both anti-Bcl-2 and anti-GFP antibodies (Fig. 1B). Transiently over-expressed GFP-Bcl-2 migrated at the expected molecular mass, and the transient transfection protocol resulted in substantially higher levels of Bcl-2 compared to endogenous Bcl-2 in HEK-293 cells (which required a longer exposure for visualisation, indicating low expression levels; Fig. 1Bii). A lower molecular weight band was also detected using the Bcl-2 antibody, which migrated at approximately the same mass as endogeneous Bcl-2. Since this was not detected in GFP-transfected cells, it is likely that it was due to proteolysis of the GFP-Bcl-2 fusion protein. Using FACS analysis to detect GFP positive cells, it was evident that ~40% of the transiently transfected cell population expressed GFP-Bcl-2, and that the levels of

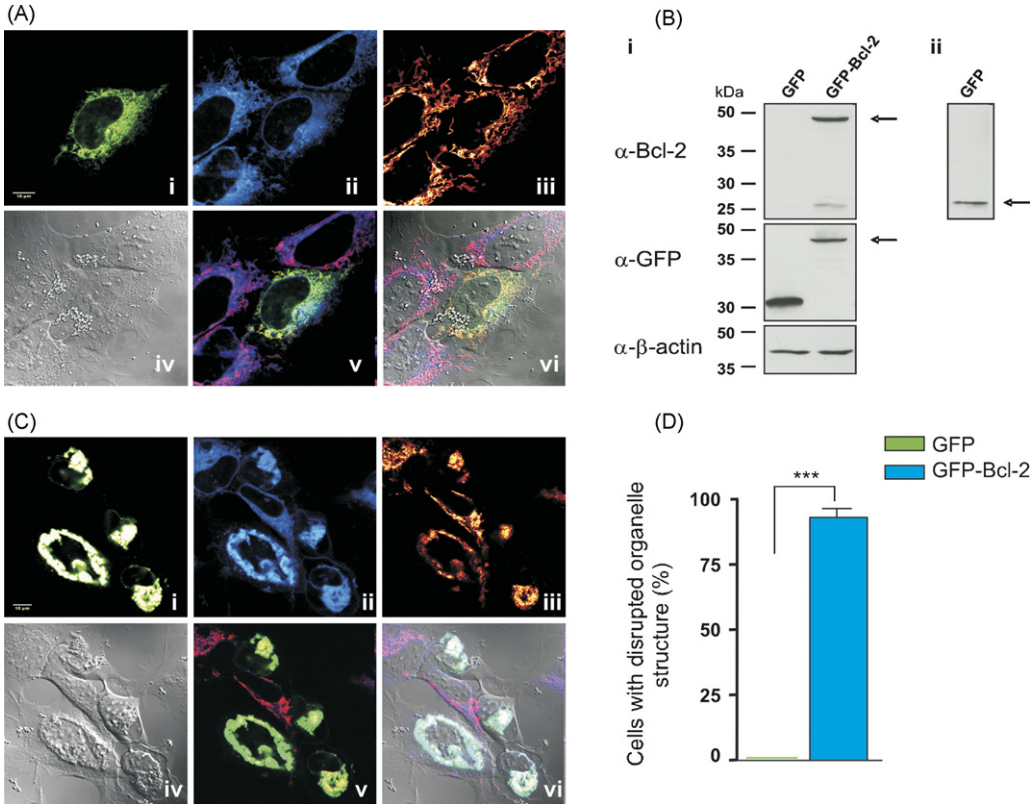

Figure 1 Localisation and expression of transiently transfected GFP-Bcl-2, and its effect on organelle structure. HEK-293 cells were imaged or harvested 16 h post-transfection. (A) Representative confocal images of cells transiently transfected with GFP-Bcl-2. (Ai) GFP-Bcl-2 fluorescence. (Aii) Cells were loaded with ER-Tracker Blue-White DPX to illustrate ER structure and (Aiii) TMRE to highlight mitochondrial structure. (Aiv) Transmitted light DIC image. (Av) GFP/ER-Tracker/TMRE overlay. (Avi) GFP/ER-Tracker/TMRE/DIC overlay. Scale bar = 10 μm. (Bi) over-expression of GFP-Bcl-2 was confirmed by immunoblotting of total cell lysates with anti-Bcl-2 and anti-GFP antibodies (see arrows). β-actin was used as a loading control. (Bii) A longer exposure of control cells confirmed the presence of endogenous Bcl-2 (see arrow). Blots are representative of at least 3 experiments. (C) Representative confocal images of cells transiently transfected with GFP-Bcl-2 showing disrupted organelle structure. (Ci) GFP-Bcl-2 fluorescence. (Cii) Cells were loaded with ER-Tracker Blue-White DPX to illustrate ER structure and (Ciii) TMRE to highlight mitochondrial structure. (Civ) Transmitted light DIC image. (Cv) GFP/ER-Tracker/TMRE co-localisation overlay. (Cvi) GFP/ER-Tracker/TMRE/DIC co-localisation overlay. Scale bar = 10 μm. (D) Using confocal microscopy, fields of view were scored for cells with abnormal organelle structure. Data represents the mean ± S.E.M. of at least 30 fields of cells per coverslip, from 3 independent coverslips per day, on 3 individual days. Statistical significance is denoted by ($^{***}p < 0.001$).

GFP fluorescence, which correspond with Bcl-2 expression levels, varied greatly (Fig. 4D).

3.2. Transiently over-expressed Bcl-2 disrupts organelle structure

During examination of the cells transiently transfected with the GFP-Bcl-2 expression vector, it became obvious that a large proportion (93 ± 3%) of the cells contained aggregates of GFP-Bcl-2, and had disrupted organelle morphology. Overlays of GFP-Bcl-2 fluorescence and specific organelle markers showed that both the ER and mitochondrial structures were affected. This is evident in Fig. 1C, which shows that all the cells expressing GFP-Bcl-2 (the green cells in panel Ci) had both compromised ER (panel Cii) and mitochondria (panel Ciii). Expression of GFP alone did not affect organelle morphology (Fig. 1D). Additional experiments,

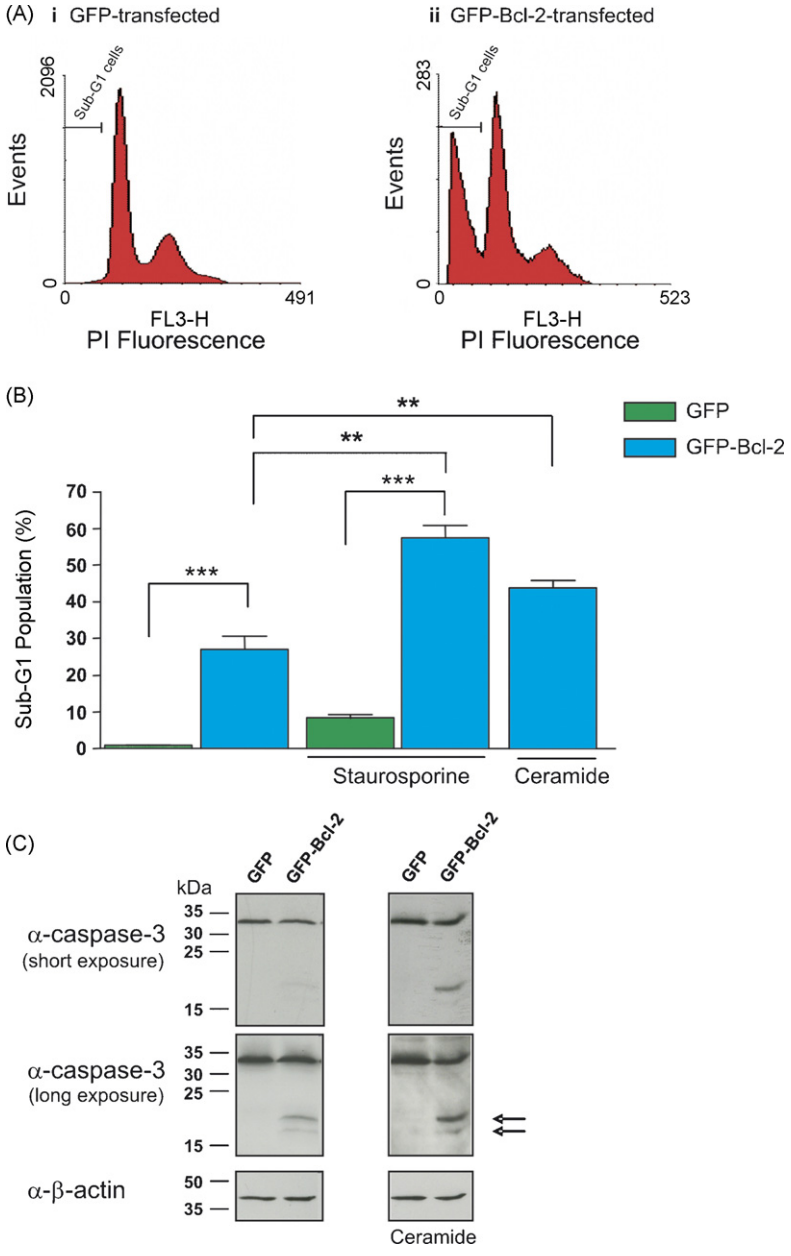

Figure 2 Transient transfection of GFP-Bcl-2 induces apoptosis and sensitises cells to apoptotic stimuli. HEK-293 cells were treated with staurosporine (4 μM; 4 h) or ceramide (30 μM; 16 h) as indicated. Cells were harvested 16 h post-transfection. (A and B) The proportion of cells with sub-G1 DNA content was determined by FACS analysis of PI-stained cells. (A) Representative frequency histograms of (Ai) GFP-transfected cells and (Aii) GFP-Bcl-2-transfected cells. (B) Sub-G1 data is represented as the mean ± S.E.M. of at least 3 individual experiments. Statistical significance is denoted by ($^{**}p < 0.01$) and ($^{***}p < 0.001$). (C) Caspase-3 activation was examined by immunoblotting of total cell lysates with an anti-caspase-3 antibody, with both short (top) and long (bottom) exposures shown, arrows indicate cleaved caspase-3. β-actin was used as a loading control. The blots are representative of at least 3 experiments.

carried out in HeLa cells, and caspase-9 dominant-negative lung epithelial (IMR-90) cells, showed that transiently over-expressed GFP-Bcl-2 disrupted organelle structure in a similar proportion of cells, indicating that the effect of Bcl-2 was not cell type specific (data not shown). To rule out adverse effects of specific transfection reagents, GeneJuice (Novagen; cellular protein and novel polyamine), JetPEI (Qbiogene; linear polyethylenemine) and Lipofectamine 2000 (Invitrogen; cationic lipid formulation) were all used to transiently transfect GFP-Bcl-2. Similar results were seen independent of the transfection reagent employed (data not shown). In order to determine whether the GFP tag at the NH_2-terminus was contributing to the damaging effects of transiently over-expressed GFP-Bcl-2, an untagged version of Bcl-2 and a Bcl-2 construct with monomeric red fluorescent protein appended to the NH_2-terminus (RFP-Bcl-2) were employed. Similarly to GFP-Bcl-2, untagged Bcl-2 and RFP-Bcl-2 caused disruption of organelle structure (data not shown).

3.3. Transiently over-expressed Bcl-2 functions in a pro-apoptotic manner

In addition to changes in organelle morphology, HEK-293 cells transiently transfected with Bcl-2 were observed to become rounded-up and detach from the coverslips, in contrast to the characteristically flat adherent control cells. Furthermore, the Bcl-2-transfected cells displayed morphological features of apoptosis, including cell shrinkage and blebbing. To quantitate the putative induction of apoptosis more precisely, flow cytometry was used to measure DNA fragmentation, which is manifest as an increase in the number of cells having a DNA content below that observed in cells in the G1 phase of the cell cycle (i.e. sub-G1). For this purpose, DNA was stained in fixed cells with propidium iodide (PI). Our results clearly indicated that a significant proportion of cells transiently over-expressing GFP-Bcl-2, selected by FACS, were apoptotic. This is evident in Fig. 2A, which illustrates the difference in DNA content between HEK-293 cells transfected with either GFP alone (panel Ai) or GFP-Bcl-2 (panel Aii). The large sub-G1 peak in the GFP-Bcl-2-expressing cells indicates a significant induction of apoptosis. Moreover, in addition to causing cell death, transient transfection of GFP-Bcl-2 sensitised the cells to the pro-apoptotic stimuli ceramide and staurosporine. Application of staurosporine (4 μM; 4 h) or ceramide (30 μM; 16 h) to the GFP-Bcl-2-transfected cells increased the proportion of sub-G1 cells, from $27 \pm 3\%$ in controls, to 58 ± 4 and $44 \pm 2\%$, respectively (Fig. 2B). These data indicate that not only was GFP-Bcl-2 pro-apoptotic when transiently over-expressed but it also sensitised cells to the effects of apoptotic inducers.

Though PI staining is a widely used assay for detecting apoptotic cells, cellular DNA can be decreased through other processes than apoptosis, such as necrosis [22]. To further corroborate the sub-G1 data, we examined the integrity of caspase-3, which is cleaved and activated by upstream caspases (e.g. caspase-8 and caspase-9). Caspase 3 is an 'executioner' protease that is responsible for many of the caspase-dependent events, such as EndoG cleavage, required for apoptosis to progress. Total cell lysates from cells transiently over-expressing GFP-Bcl-2, were resolved by SDS-PAGE and immunoblotted using an anti-caspase-3 antibody, which detects both the inactive (~32 kDa) and the active proteolytically processed protein (one or more fragments between 14 and 21 kDa). In agreement with the sub-G1 DNA content data, cleaved caspase-3 was detected in cells transiently over-expressing GFP-Bcl-2 (Fig. 2C). Treatment with staurosporine or ceramide increased the appearance of active caspase-3 in the GFP-Bcl-2-transfected cells. The cell death induced by transient over-expression of GFP-Bcl-2 was prevented using the competitive irreversible cell-permeant caspase inhibitor zVAD-FMK. FACS analysis of sub-G1 DNA in PI-stained cells 16 h post-transfection with GFP-Bcl-2 revealed that zVAD-FMK (10 μM; 16 h) reduced the proportion of cells undergoing apoptosis from $27 \pm 3\%$ to $4 \pm 0.6\%$ ($n = 3$). Furthermore, zVAD-FMK prevented the cleavage of caspase-3 following transient transfection of Bcl-2 (data not shown). These data confirmed that transient transfection of Bcl-2 induced apoptotic cell death in a caspase-dependent manner.

3.4. Localisation and expression of stably over-expressed GFP-Bcl-2

Since, in our hands, transient transfection of Bcl-2 caused cell death and sensitised cells to pro-apoptotic stimuli, we explored the effects of stably expressing Bcl-2 (see Section 2 for generation of stable cells). Live-cell confocal imaging was used to assess the sub-cellular distribution of GFP-Bcl-2 in the stable clones. GFP-Bcl-2 co-localised with the ER marker, ER-Tracker Blue-White DPX, and the mitochondrial marker, TMRE, indicating correct sub-cellular localisation (Fig. 3A). Over-expression was confirmed by resolving total cell lysates, using SDS-PAGE, and immunoblotting with anti-GFP and anti-Bcl-2 antibodies (Fig. 3B). Flow cytometry revealed that 100% of cells were positive for green fluorescence, and thus expressing GFP-Bcl-2. Observation of cells stably over-expressing GFP-Bcl-2, using confocal microscopy, showed that significantly fewer cells had disrupted organelle structure and that the disruption appeared to be less severe. Only $33 \pm 3\%$ of cells exhibited organelle disruption, which was almost three-fold lower than that observed when GFP-Bcl-2 was transiently over-expressed (Fig. 3C). Furthermore, the DIC images revealed that the cells were not rounding-up or blebbing, and therefore not dying.

3.5. Stably over-expressed Bcl-2 functions in an anti-apoptotic manner

To determine whether stably over-expressed GFP-Bcl-2 could function in an anti-apoptotic manner, levels of sub-G1 DNA and caspase-3 cleavage were examined. Stable expression of GFP-Bcl-2 did not induce apoptosis, as the proportion of cells displaying sub-G1 DNA content was <3%, which was equivalent to that observed in control GFP expressing cells. Furthermore GFP-Bcl-2 expressing cells were protected from staurosporine-induced apoptosis, indicating that Bcl-2 was functioning correctly (Fig. 3D). Unlike transient expression of GFP-Bcl-2, stable introduction of the protein did

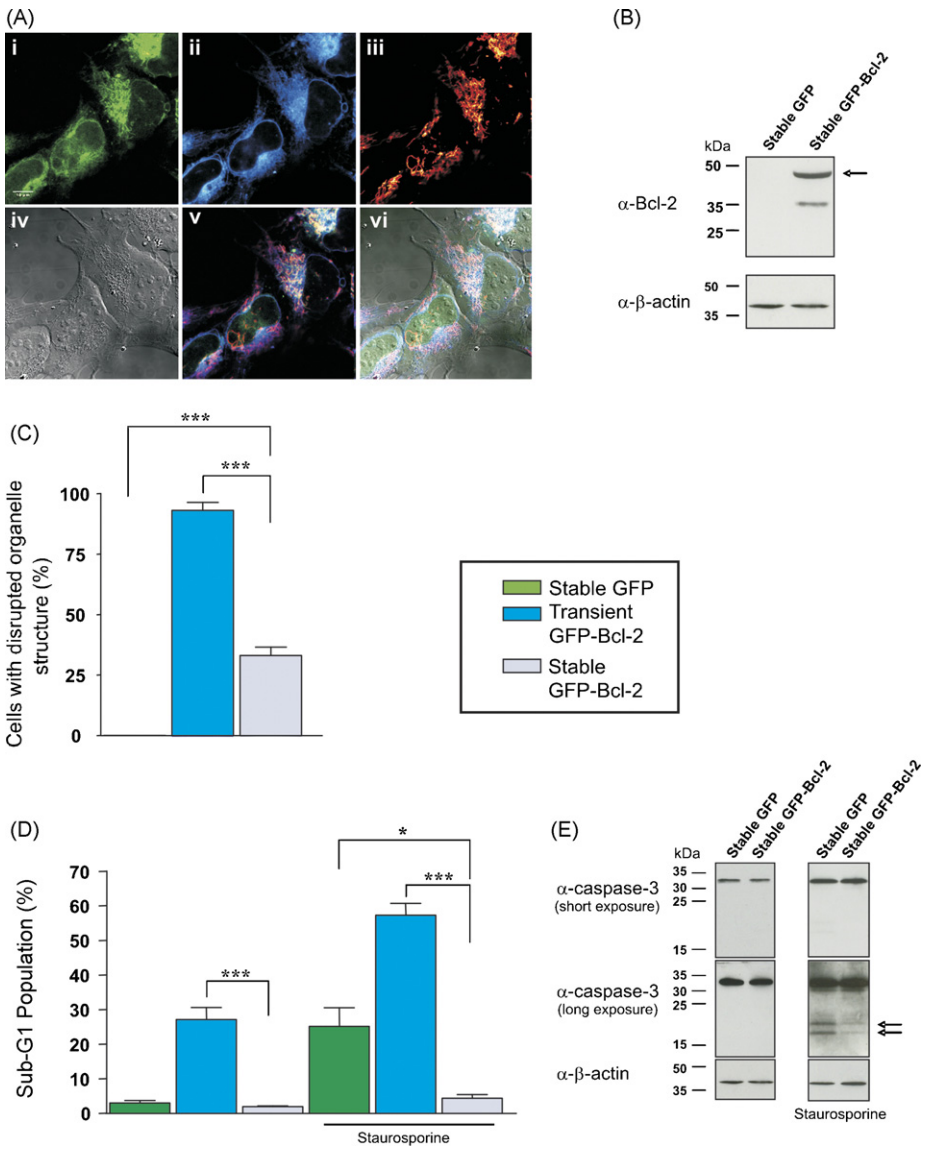

Figure 3 Localisation of stably transfected GFP-Bcl-2, which functions in an anti-apoptotic manner. HEK-293 cells stably expressing GFP-Bcl-2 were either imaged or harvested for immunoblotting. (A) Representative confocal images of cells stably over-expressing GFP-Bcl-2. (Ai) GFP-Bcl-2 fluorescence. (Aii) Cells were loaded with ER-Tracker Blue-White DPX to illustrate ER structure and (Aiii) TMRE to highlight mitochondrial structure. (Aiv). Transmitted light DIC image. (Av) GFP/ER-Tracker/TMRE overlay. (Avi) GFP/ER-Tracker/TMRE/DIC overlay. Scale bar = 10 μm. (B) over-expression of GFP-Bcl-2 was confirmed by immunoblotting total cell lysates with anti-Bcl-2 (see arrow). β-actin was used as a loading control. Blots are representative of at least 3 experiments. (C) Using confocal microscopy, fields of view were scored for cells with disrupted organelle structure. Data represents the mean ± S.E.M. of at least 30 fields per coverslip, from 3 independent coverslips per day, on 3 individual days. The corresponding data obtained from cells transiently transfected with the GFP-Bcl-2 expression vector is presented for comparison. (D) The proportion of cells with sub-G1 DNA content was determined by FACS analysis of PI-stained cells. Sub-G1 data is represented as the mean ± S.E.M. of at least 3 individual experiments. The corresponding data obtained from cells transiently transfected with GFP-Bcl-2 is presented for comparison. (E) Caspase-3 activation was examined by immunoblotting total cell lysates using an anti-caspase-3 antibody, with a short (top) and long (bottom) exposure as shown. Arrows indicate cleaved caspase-3. β-actin was used as a loading control. Blots are representative of at least 3 experiments. Statistical significance is denoted by ($^{*}p < 0.05$) and ($^{***}p < 0.001$).

not cause caspase-3 cleavage in control cells. Also, the stable expression of GFP-Bcl-2 reduced the cleavage of caspase-3 normally observed in cells in which apoptosis had been induced with staurosporine (Fig. 3E). These data indicate that stable expression of Bcl-2 protected cells from apoptosis.

3.6. Higher levels of Bcl-2 expression are achieved upon transient transfection, compared to stable transfection

It is established that the concentration of a heterologously expressed protein is generally higher following transient

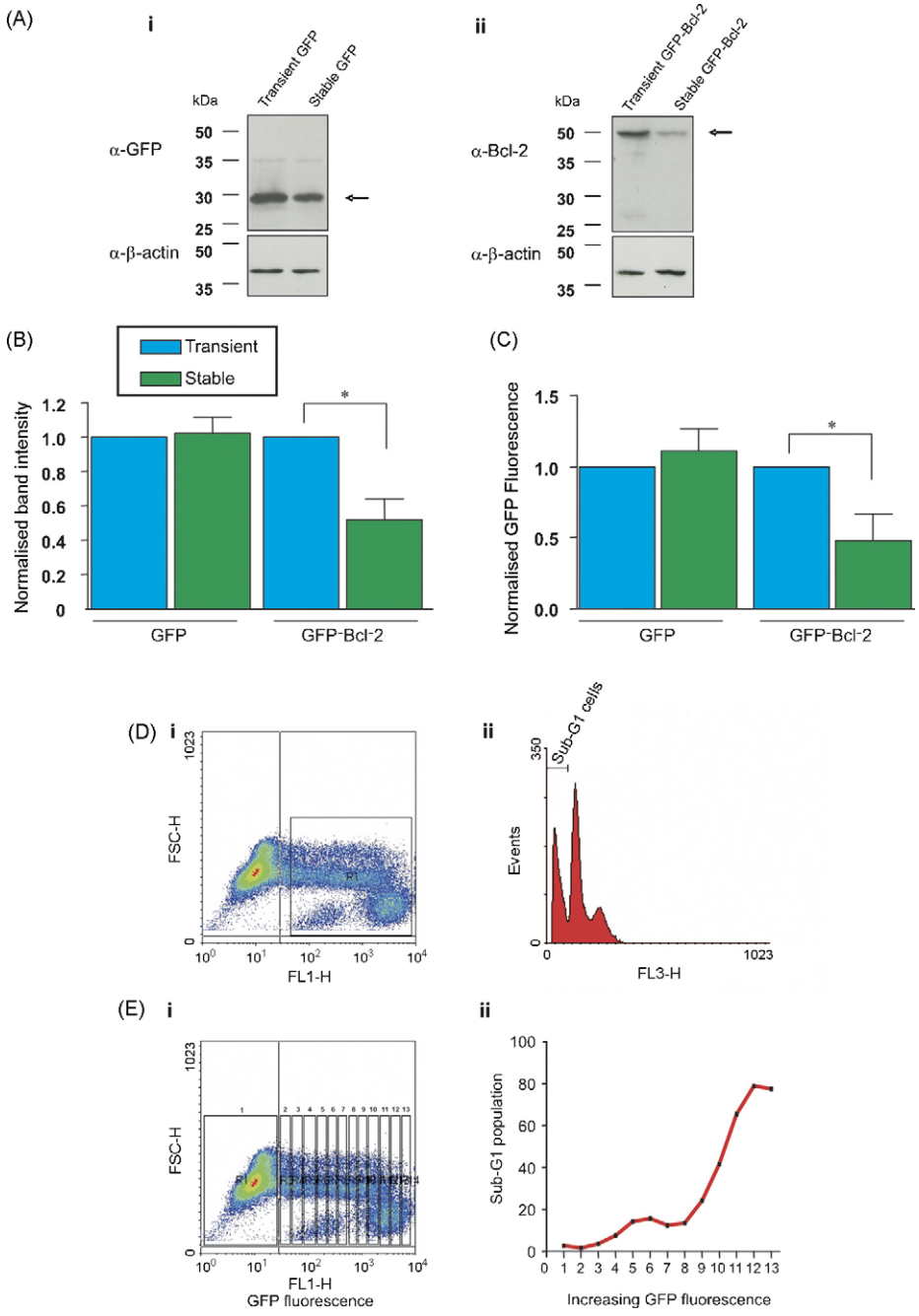

Figure 4 Transiently transfected GFP-Bcl-2 expresses at a higher level than stably transfected GFP-Bcl-2, and its magnitude of expression correlates with apoptosis. HEK-293 cells were stably or transiently (16 h) transfected with expression vectors for GFP or GFP-Bcl-2. (A) Expression levels were compared by immunoblotting of total cell lysates, normalised for protein content, with (Ai) anti-GFP or (Aii) anti-Bcl-2 antibodies (see arrows). β-actin was used as a loading control. Blots are representative of at least 3 experiments. (B) The band intensity from immunoblots was normalised to the mean intensity of the transient populations. (C) Fluorescence of cell populations, analysed using FACS, was normalised to the mean fluorescence of the transient populations. (D and E) HEK-293 cells were harvested 16 h post-transfection with GFP-Bcl-2. The proportion of cells with sub-G1 DNA content was determined by FACS analysis of PI stained cells. (Di) Representative density plot of GFP fluorescence. R1 indicates gated cells. (Dii) Corresponding frequency histogram of cells with sub-G1 DNA in the gated R1 region. (Ei) Same density plot as in Ai, but with the population of GFP-positive cells segmented into smaller regions (labelled 2—13). (Eii) Analysis of sub-G1 DNA content in the cells within the regions indicated in Ei. The data are representative of 3 independent experiments. Data represent the mean ± S.E.M. of at least 3 individual experiments, with statistical significance denoted by ($^*p < 0.05$).

transfection than with stable transfection. We therefore examined whether GFP-Bcl-2 was indeed expressed at higher levels following transient transfection of HEK-293 cells, compared to their stably over-expressing counterparts, and whether higher levels of expression correlated with pro-apoptotic behaviour. From immunoblots of total cell lysates normalised for protein content, it was evident that with stable transfection Bcl-2 was expressed at a significantly lower level than following transient transfection (Fig. 4A and B). Since the stable GFP-Bcl-2-expressing cell lines cells were continually grown in selection medium, the entire population was positive for GFP-Bcl-2. In contrast, since Lipofectamine 2000 is not 100% effective, a proportion of the cells that had undergone transient transfection did not express GFP-Bcl-2 (Figs. 1 and 4). Considering that some of the Lipofectamine-treated cells would not have been transfected, the differences between stable and transient GFP-Bcl-2 cells would have been even greater than that shown in Fig. 4A and B. Similar differences in GFP-Bcl-2 expression were observed using FACS analysis of GFP fluorescence. This approach allows selection of GFP positive cells (and thus only GFP-Bcl-2-expressing cells), and measures absolute fluorescence levels per individual cell, giving a more reliable representation. The results corroborated those obtained using immunoblotting, showing that the mean fluorescence was significantly lower in cells stably over-expressing GFP-Bcl-2 compared to populations of transiently transfected cells (Fig. 4C). These data confirm that higher levels of GFP-Bcl-2 are achieved upon transient over-expression.

To determine whether there was a direct correlation between the expression level of GFP-Bcl-2 and apoptosis, a combined analysis of sub-G1 DNA and GFP-Bcl-2 fluorescence intensity was undertaken using FACS. Taking a whole population of transiently transfected cells indicated that 29% of the cells had sub-G1 DNA (Fig. 4D). However, if the same population of cells was analysed on the basis of increasing GFP-Bcl-2 expression, then it became obvious that the proportion of cells with sub-G1 DNA was augmented in a supra-linear manner (Fig. 4E). It therefore appears that higher expression levels of Bcl-2 make its pro-apoptotic behaviour more prominent.

3.7. Manipulation of Bcl-2 expression levels using the TREx system

The data presented above suggest that high levels of Bcl-2 expression, generated by transient transfection, are pro-apoptotic. Whereas, the lower levels of Bcl-2 expression obtained during selection of cells stably expressing Bcl-2 cells are anti-apoptotic. In order to rule out differences due to expression paradigm (transient versus stable), a system was used where expression levels could be manipulated using the same cell line and same method of transfection. To this end, the Tetracycline Regulated Expression (T-REx) inducible system was used. T-REx-293 cells stably over-express a tetracycline repressor which allows for repression and de-repression of a modified CMV promoter containing Tet operator (TO) sequences. This allows expression of genes contained within a pcDNA4/TO backbone to be precisely regulated [19]. For this purpose, Bcl-2 cDNA from pB4-Bcl-2 was sub-cloned into the pcDNA4/TO-GFP expression vector yielding pcDNA4/TO-GFP-Bcl-2, which is an inducible form of GFP-Bcl-2, termed TO-GFP-Bcl-2. To over-express GFP-Bcl-2 in TREx-293 cells, transfection of the TO-GFP-Bcl-2 vector and induction with doxycycline (1 μg/ml; 16 h) are required (note that the protein expressed by the TO-GFP-Bcl-2 vector is GFP-Bcl-2; the term 'TO-GFP-Bcl-2' simply relates to its regulation by doxycycline).

The essential benefit of the T-REx system for this study is that upon transient transfection and induction (with doxycycline), high levels of GFP-Bcl-2 expression are achieved. In contrast, upon transfection without induction expression is constitutively repressed, and a very low basal level of GFP-Bcl-2 transcription occurs. To confirm doxycycline-dependent expression of TO-GFP-Bcl-2, total cell lysates were immunoblotted with anti-Bcl-2 and anti-GFP antibodies (Fig. 5A). TO-GFP-Bcl-2 migrated at the expected molecular weight, and was sensitive to doxycycline induction. Without application of doxycycline, TO-GFP-Bcl-2 transfection evoked a much lesser expression of GFP-Bcl-2 (Fig. 5A). Comparison of band intensity confirmed that there was a significantly lower level of expression in cells where expression had not been induced with doxycycline (Fig. 5B). To corroborate these data, flow cytometry was used to compare GFP fluorescence levels. A significantly lower level of GFP fluorescence was recorded in TO-GFP-Bcl-2-transfected cells in the absence of doxycyline, compared to cells where expression had been induced (Fig. 5C). The T-Rex system therefore provided a suitable system to modulate the expression of Bcl-2, whilst using the same transfection method.

3.8. Localisation and expression of transiently over-expressed TO-GFP-Bcl-2

Confocal microscopy was used to examine the sub-cellular localisation of TO-GFP-Bcl-2 in TREx-293 cells. The fluorescent dye ER-Tracker Blue-White DPX was used to highlight the ER, and TMRE was used to illustrate mitochondria. Fig. 5D and E depict the localisation of TO-GFP-Bcl-2 in cells without induction (panel D; no doxycycline; low level of GFP-Bcl-2) or with induction (panel E; 1 μg/ml doxycycline for 16 h; high levels of GFP-Bcl-2). It is evident that TO-GFP-Bcl-2 was correctly localised to both ER and mitochondrial membranes in the induced and non-induced cells. However, there was a significant difference in the appearance of the cells in which TO-GFP-Bcl-2 had been induced. Using the same settings for confocal image capture, it was evident that the induced cells had greater GFP-Bcl-2 expression and that the protein was concentrated into dense perinuclear aggregates. Furthermore, the specific organelles markers indicated that these structures were disrupted. These observations are presented in a quantitative manner in Fig. 5F. It is evident that cells transfected with TO-GFP-Bcl-2 and induced with doxycycline had similar levels of organelle disruption as cells transiently transfected with the GFP-Bcl-2 used earlier in this study (i.e. in Figs. 1—4). Cells in which GFP-Bcl-2 was stably expressed, or following transient

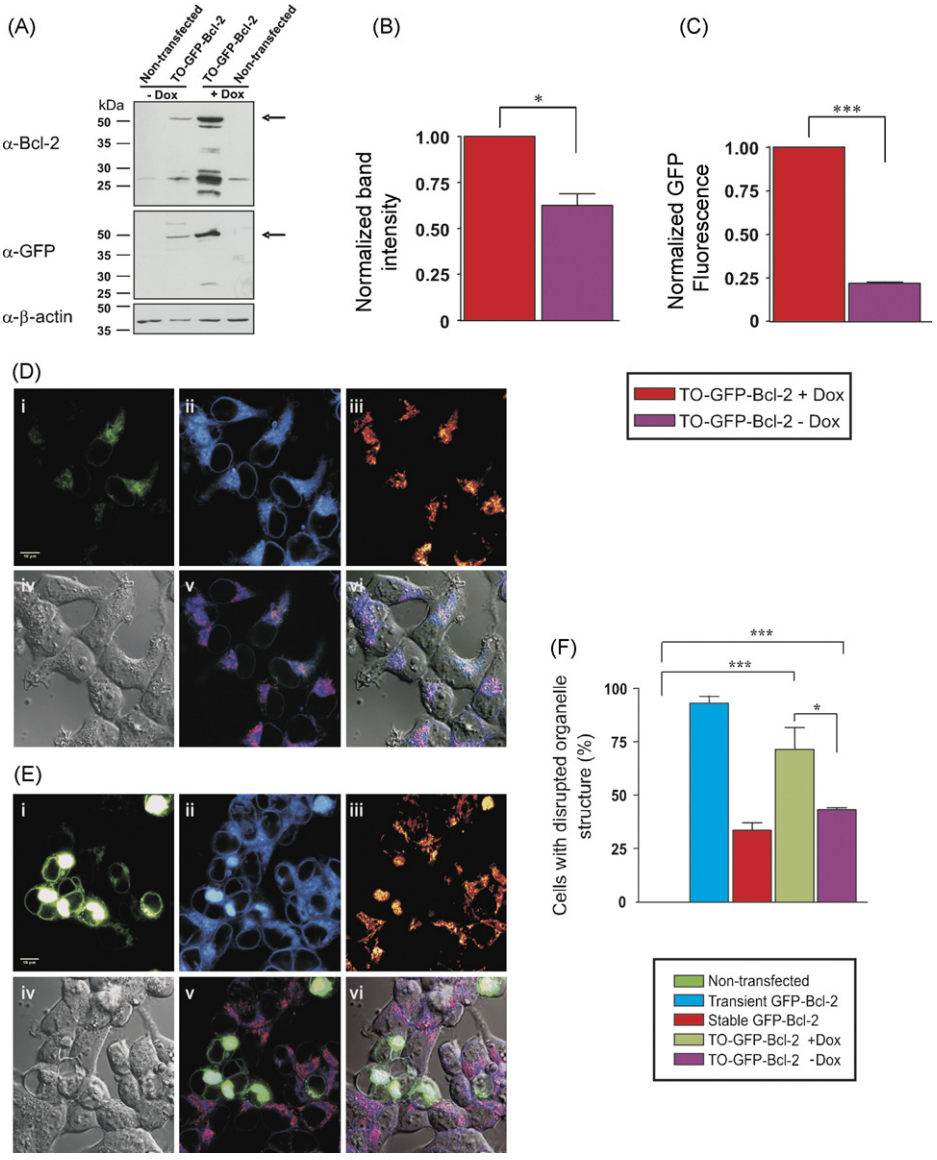

Figure 5 Higher levels of TO-GFP-Bcl-2 expression in TREx-293 cells are achieved upon doxycycline induction, and can disrupt organelle structure. TREx-293 cells were treated with or without doxycycline (1 μg/ml; 16 h), as shown, and were harvested 16 h post-transfection. (A) Expression of TO-GFP-Bcl-2 was confirmed by immunoblotting of total cell lysates, normalised for protein content, with anti-Bcl-2 and anti-GFP antibodies (see arrows). β-actin was used as a loading control. Blots are representative of at least 3 experiments. (B) The band intensity from immunoblots was normalised to the mean intensity of induced populations. (C) Fluorescence of cell populations, analysed using FACS, was normalised to the mean fluorescence of induced populations. Data is represented as the mean ± S.E.M. of at least 3 individual experiments. (D—F) TREx-293 cells treated with or without doxycycline (1 μg/ml; 16 h), were imaged 16 h post-transfection. (D and E) Representative confocal images of cells. (Di) TO-GFP-Bcl-2 expression was not induced, the cells therefore show normal organelle structure. (Ei) TO-GFP-Bcl-2 expression was induced, and the cells have disrupted organelle structure. (Dii and Eii) Cells were loaded with ER-Tracker Blue-White DPX to illustrate ER structure and (Diii, Eiii) TMRE to highlight mitochondrial structure. (Div and Eiv) Transmitted light DIC image. (Dv and Ev) GFP/ER-Tracker/TMRE overlay. (Dvi and Evi) GFP/ER-Tracker/TMRE/DIC overlay. Scale bar = 10 μm. (F) Using confocal microscopy, fields of view were scored for cells with disrupted organelle structure. Data represent the mean ± S.E.M. of at least 30 fields per coverslip, using at least 3 coverslips per day, on 3 individual days. The corresponding data from cells transiently and stably transfected with GFP-Bcl-2 data is presented for comparison. Statistical significance is denoted by ($^{*}p < 0.05$) and ($^{***}p < 0.001$).

transfection with TO-GFP-Bcl-2 in the absence of doxycycline, still showed some organelle disruption, but it was significantly less common (Fig. 5F). Furthermore, empirical observation of the cells suggested that the extent of organelle disruption was milder.

3.9. Induction of TO-GFP-Bcl-2 expression induces apoptosis

We next determined whether the level of TO-GFP-Bcl-2 expression influenced cell survival, independent of

transfection paradigm. Cells transiently transfected with TO-GFP-Bcl-2, but where expression had not been induced by doxycycline, showed low levels of spontaneous death (sub-G1 DNA content; $2 \pm 0.7\%$), similar to that observed in control cells. Whereas, those cells transiently transfected with TO-GFP-Bcl-2 in which expression had been induced showed a significantly higher proportion of cells with sub-G1 DNA content ($18 \pm 2\%$) (Fig. 6A). The proportion of cell death following transient transfection with TO-GFP-Bcl-2 with induction was similar to that observed in cells transiently transfected with GFP-Bcl-2 (Fig. 2B). Incubation with staurosporine (4 μM; 4 h) significantly increased the fraction of cells that were apoptotic in all cases, but produced a dramatic elevation of cell death in cells where TO-GFP-Bcl-2 expression had been induced by doxycycline (Fig. 6A). A similar effect was observed when monitoring cleavage of caspase 3 as a marker of apoptosis induction. Active (cleaved) caspase-3 was not detectable in cells where TO-GFP-Bcl-2 expression had not been induced, but following doxycycline incubation cleaved caspase-3 was evident (Fig. 6B). These data support the results shown earlier and suggest that higher levels of Bcl-2 expression promote greater induction of apoptosis, even when using the same expression paradigm.

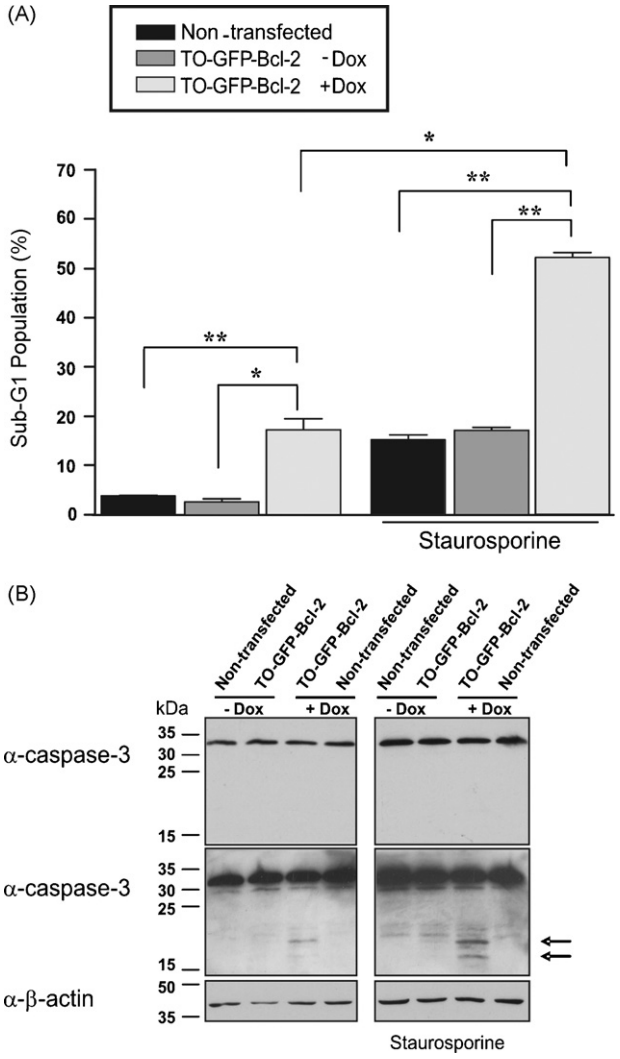

Figure 6 High level of TO-GFP-Bcl-2 expression, due to induction with doxycyline, causes apoptosis and sensitises cells to apoptotic stimuli. TREx-293 cells were treated with doxycycline (1 μg/ml; 16 h) or staurosporine (4 μM; 4 h) as shown. Cells were harvested 16 h post-transfection. (A) The proportion of cells with sub-G1 DNA content was determined by FACS analysis of PI stained cells. Sub-G1 data is represented as the mean ± S.E.M. of at least 3 individual experiments. Statistical significance is denoted by ($^{*}p < 0.05$) and ($^{**}p < 0.01$). (B) Caspase-3 activation was examined by immunoblotting of total cell lysates with an anti-caspase-3 antibody, with a short (top) and long (bottom) exposure shown, arrows indicate cleaved caspase-3. β-actin was used as a loading control. Blots are representative of at least 3 experiments.

Cells stably expressing GFP-Bcl-2 and those transiently transfected with TO-GFP-Bcl-2 (without induction) had similar amounts of Bcl-2. However, unlike stable Bcl-2 expression, the low level of TO-GFP-Bcl-2 obtained without induction did not protect against apoptosis. As described above, TO-GFP-Bcl-2 did not cause spontaneous apoptosis without doxycycline induction, but it did not prevent staurosporine-induced apoptosis either (Fig. 6A). It appears that the same concentration of Bcl-2 is more efficacious in inhibiting cell death if it has been constitutively expressed in a cell, rather than transiently introduced.

3.10. Bcl-2 disrupts organelle structure and induces apoptosis in a Ca^{2+}-dependent manner

The severe fragmentation of cellular organelles and induction of apoptosis by Bcl-2 is surprising given the well-known pro-survival role of this protein. We sought to probe the mechanisms by which high levels of Bcl-2 can deleteriously affect cell ultrastructure. Our initial experiments examined the potential role of Ca^{2+} in this process, since it has been previously shown that acutely elevated cytosolic Ca^{2+} concentrations cause organelle disruption [23—25]. To visualise organelles, HEK-293 cells were co-transfected with EGFP and DsRed targeted to the ER and mitochondria, respectively. The cells were then incubated with 10 μM ionomycin for 2 h and visualised using confocal microscopy. Similar to the effect of transient Bcl-2 expression, the treatment with ionomycin caused disruption to the ER and mitochondrial structure (Fig. 7A).

To determine whether Ca^{2+} was playing a role in the Bcl-2-induced organelle disruption and cell death observed in this study, two approaches were adopted. The first was to reduce $InsP_3$-evoked Ca^{2+} release, and the second was to buffer cytosolic calcium. The Ca^{2+}-mobilising action of $InsP_3$ can be prevented by expressing the inositol 1,4,5-trisphosphate 5′-phosphatase enzyme ($InsP_3$ 5′Pase), which dephosphorylates $InsP_3$ to inositol 1,4-bisphosphate ($InsP_2$). $InsP_3$Rs are not activated by $InsP_2$, and we have observed that agonist-mediated Ca^{2+} release is completely abrogated by introduction of $InsP_3$ 5′pase (unpublished observations). HEK-293 cells were transiently transfected with GFP-Bcl-2 and $InsP_3$ 5′Pase and examined using confocal microscopy. As depicted in Fig. 7B, the presence of the $InsP_3$ 5′Pase significantly lowered the proportion of GFP-Bcl-2-expressing cells exhibiting abnormal organelle structure, compared to those

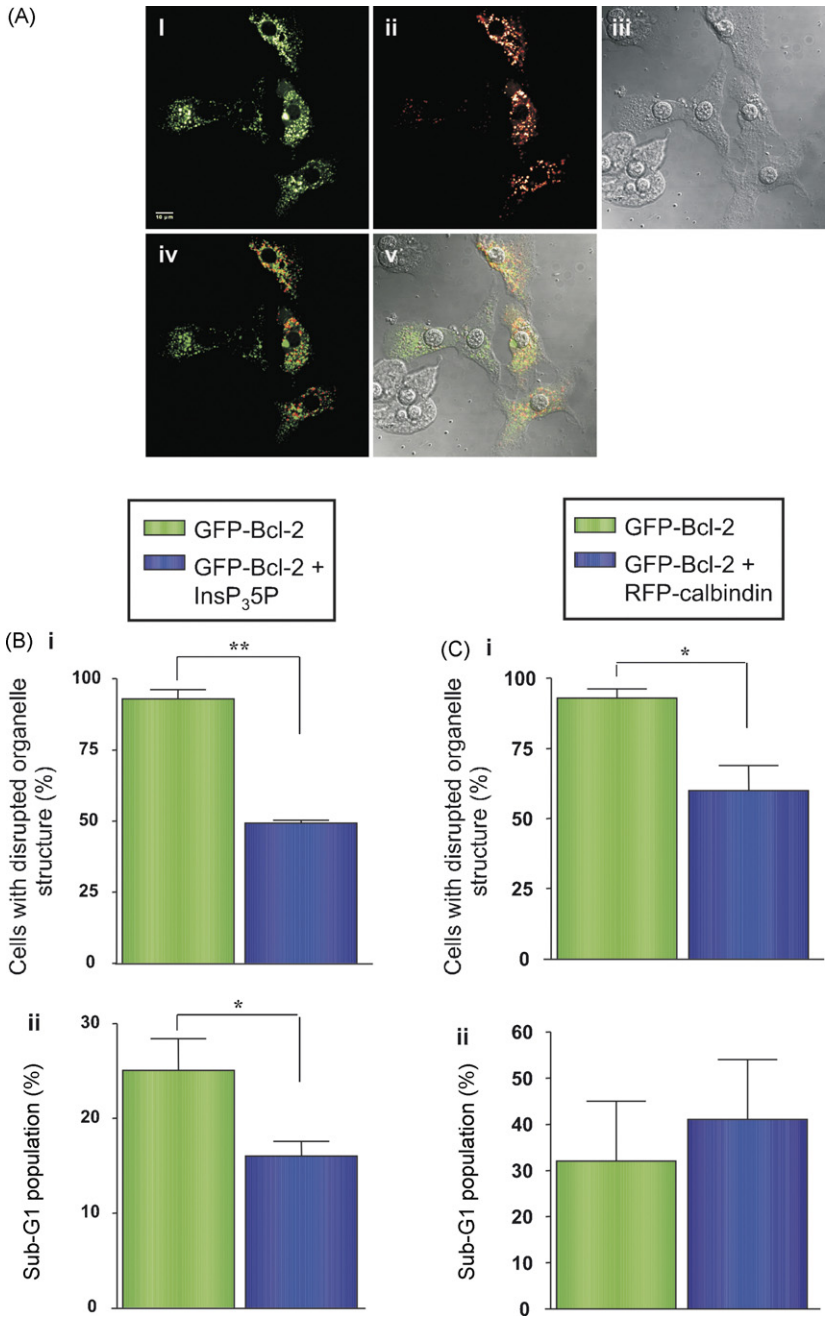

Figure 7 Ca^{2+}-dependent apoptosis caused by ionomycin or Bcl-2 provokes organelle fragmentation. (A) Representative confocal images of HEK-293 cells treated with ionomycin (10 μM; 2 h). (Ai) Cells were transfected with GFP-ER to illustrate ER structure and (Aii) DsRed-Mito to highlight mitochondrial structure. (Aiii) A transmitted light DIC image was taken simultaneously. (iv) GFP/DsRed overlay. (v) GFP/DsRed/DIC co-localisation overlay. The cells were imaged 24 h post-transfection. Scale bar = 10 μm. (Bi and Ci) HEK-293 cells were imaged or harvested 16 h post-transfection with the constructs denoted by the columns (note that the InsP3 5′ phosphatase is denoted as InsP35P). Using confocal microscopy, fields of view were scored for cells with disrupted organelle structure. Data represent the mean ± S.E.M. of at least 30 fields per coverslip from 3 coverslips per day on 3 individual days. (Bii and Cii) The proportion of cells with sub-G1 DNA content was determined by FACS analysis of PI stained cells. Sub-G1 data is represented as the mean ± S.E.M. of at least 3 individual experiments. Statistical significance is denoted by ($^{*}p < 0.05$) and ($^{**}p < 0.01$).

over-expressing GFP-Bcl-2 alone. In addition to decreasing organelle fragmentation, introduction of the $InsP_3$ 5′Pase reduced the extent of apoptosis induced by transient transfection of Bcl-2 (Fig. 7Bii). It therefore appears that both the organelle disruption and cell death induced by Bcl-2 are dependent on $InsP_3R$ activation.

To directly test whether elevated cytosolic Ca^{2+} was required for the deleterious actions of transiently transfected Bcl-2, calbindin, a mobile cytosolic Ca^{2+} buffer, was transiently introduced into cells along with GFP-Bcl-2. The calbindin protein was tagged with RFP to enable identification of co-transfected cells. 16 h post-co-transfection

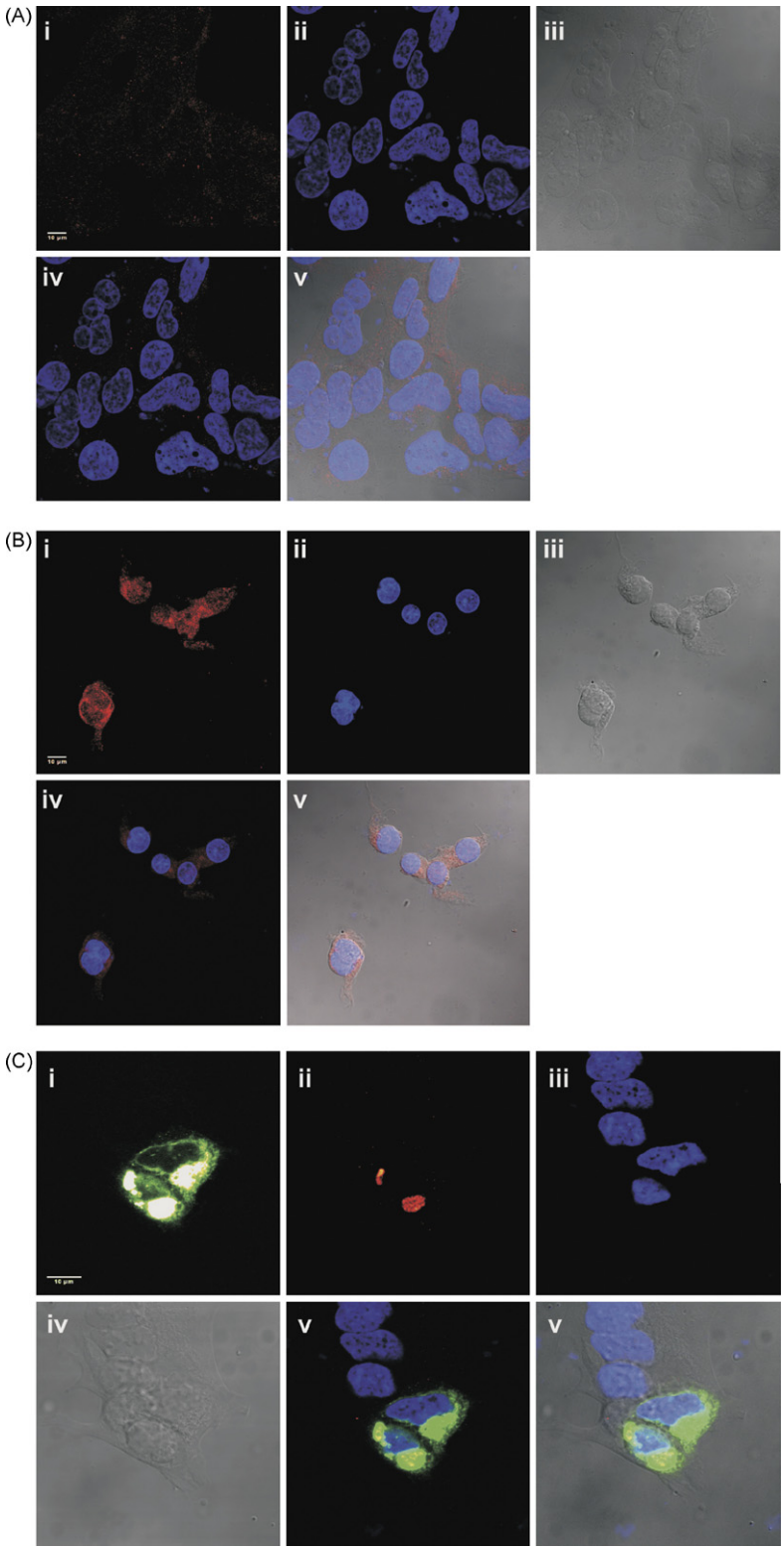

Figure 8 Lipid peroxidation occurs during ionomycin- and Bcl-2-induced apoptosis. (A and B) HEK-293 cells were treated ± ionomycin (10 μM; 2 h) and immunostained. (A and B) Representative confocal images of (A) control (untreated) cells and (B) cells treated with ionomycin. (Ai and Bi) Cells were probed with an anti-malondialdehyde antibody and (Aii and Bii) incubated with the nuclear stain, DAPI. (Aiii and Biii) A transmitted light DIC image was taken simultaneously. (Aiv and Biv) Anti-malondialdehyde/DAPI overlay. (Av and Bv) Anti-malondialdehyde/DAPI/DIC overlay. (C) Representative images of cells transiently transfected with GFP-Bcl-2 for 16 h. (Ci) GFP-Bcl-2 fluorescence. (Cii) Cells were probed with an anti-malondialdehyde antibody and (Ciii) labelled with the nuclear stain, DAPI. (Civ) A transmitted light DIC image was taken simultaneously. (Cv) GFP/anti-malondialdehyde/DAPI overlay. (Cvi) GFP/anti-malondialdehyde/DAPI/DIC overlay. Scale bar = 10 μm.

with GFP-Bcl-2 and RFP-calbindin, cell structure was examined using confocal microscopy. The presence of calbindin significantly decreased the proportion of cells with fragmented organelles, compared to those cells transiently over-expressing GFP-Bcl-2 alone (Fig. 7B). However, calbindin did not affect the induction of cell death following transient transfection of Bcl-2 (Fig. 7Bii).

3.11. Transient expression of Bcl-2 causes lipid peroxidation

The data described above suggest that Ca^{2+} released from the ER plays a role in the adverse effects of transiently expressed Bcl-2. It is known that high levels of Ca^{2+} can affect mitochondrial function leading to generation of reactive oxygen species (ROS), which can then feedback to the ER promoting further Ca^{2+} release [7,26]. Our previous work examining ionomycin-induced ER fragmentation has shown that the organelle disruption was dependent on ROS production [25]. To determine whether ROS were contributing to the destructive effects of transiently expressed Bcl-2, we examined whether lipid peroxidation, a membrane-damaging process caused by high levels of ROS, was occurring. Malondialdehyde (MDA) is an end-product of lipid peroxidation, and is readily detectable using specific antibodies [27]. As we have already observed that ionomycin can lead to generation of ROS, we used this stimulus as a positive control from the MDA assay. Cells were incubated with or without 10 μM ionomycin for 2 h, and subsequently immunostained using an anti-MDA antibody. As depicted in Fig. 8A, control cells (not treated with ionomycin) showed no sign of MDA immunoreactivity. In contrast, cells treated with ionomycin showed positive staining for MDA, indicating that ROS generation leading to lipid peroxidation had occurred (Fig. 8B). To determine whether transient expression of Bcl-2 also induced lipid peroxidation, cells were immunostained and examined using confocal microscopy, 16 h post-transfection with GFP-Bcl-2. The images in Fig. 8C indicate that cells expressing GFP-Bcl-2 had disrupted organelle structure and exhibited positive staining for MDA. Quantification of the proportion of Bcl-2-transfected cells with disrupted organelle structure and MDA immunostaining revealed that the two effects were observed together in greater than 50% of cells ($n > 100$ cells), suggesting that ROS may have contributed to the adverse effects observed when Bcl-2 was transiently expressed. To examine whether ROS was instrumental in inducing organelle fragmentation downstream of Bcl-2 introduction, the cells were incubated with the ROS scavenger, Trolox, during transient transfection period. As depicted in Fig. 9, Trolox gave a concentration-dependent protection of organelle structure from the deleterious action of transiently expressed Bcl-2.

4. Discussion

The results presented above show that transient transfection of the cDNA encoding Bcl-2 leads to a high level of protein expression. In this situation, Bcl-2 does not exhibit its classical anti-apoptotic function. Rather, it disrupts organelle structure (Fig. 1), sensitises cells to

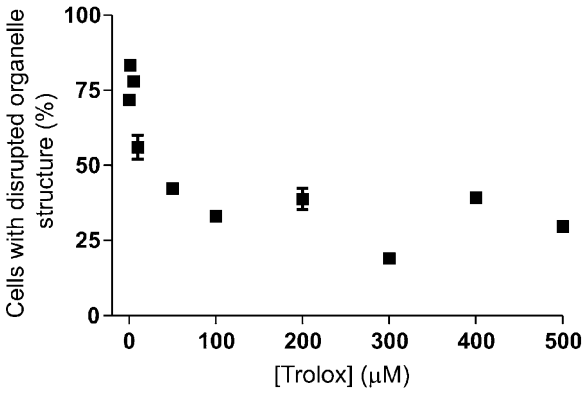

Figure 9 ROS scavenging prevents Bcl-2-induced organelle fragmentation. HEK-293 cells were transiently transfected with GFP-Bcl-2 for 16 h in the continual presence of Trolox. The proportion of cells with normal organelle structure was determined using confocal microscopy of the GFP fluorescence. The data represent mean ± S.E.M. of 3 individual experiments, with multiple cells per field of view in each experiment.

apoptotic stimuli (Fig. 2) and induces spontaneous apoptosis (Figs. 2 and 3). In contrast, stably transfected Bcl-2 is expressed at lower levels (Fig. 3) and functions in its established anti-apoptotic manner (Fig. 3). Although Bcl-2 is targeted to the correct organelles in both expression paradigms, the differing amounts of protein produced have profound, but inverse, consequences on cellular integrity.

The work described in this study was undertaken to develop a reliable cell model to explore the biology of Bcl-2. As described earlier, several groups have demonstrated that regulation of Ca^{2+} fluxes by Bcl-2 underlies its anti-apoptotic effect [8,14,28]. However, the actual effect of Bcl-2 on cellular Ca^{2+} signalling is controversial, with different laboratories proposing that the protein modulates various aspects of Ca^{2+} homeostasis or release. Our aim, therefore, was to develop a system in which Bcl-2 expression could be modulated, and the protein was correctly targeted and functioning. Our studies were carried out using HEK-293 cells, which is a reliable cell type for Ca^{2+} signalling, since they have robust and well-characterised responses to several Ca^{2+}-mobilising agonists. Furthermore, they have a low endogenous expression of Bcl-2 (Fig. 1).

Since transient transfection of Bcl-2 has been used by several groups before, it was surprising to us that is had such a drastic effect on cells. There are several advantages of transient transfection, including rapid protein expression without the need for growth in selective medium. Although it is known that transient transfection yields populations of cells with variable degrees of protein expression, it is not generally appreciated that this method also gives rise to higher average levels of Bcl-2.

Our confocal imaging observations suggest that the deleterious effects of Bcl-2 were not caused by mistargetting of the protein. Indeed, the GFP-tagged protein localised explicitly with the ER and mitochondria (Fig. 1; see also reference [4]). Rather, it appeared that high concentrations of Bcl-2 caused the apparent changes in cellular integrity. Bcl-2 is classically considered an anti-apoptotic protein, yet when expressed at a high level it caused apoptosis. The

most direct data, showing that the negative consequences of Bcl-2 correlate with the extent of expression, and are independent of transfection paradigm, was obtained using TO-GFP-Bcl-2. By introducing a doxycycline-inducible vector, we could demonstrate that the dosage of Bcl-2 was key to its pro-apoptotic activity (Fig. 5). The same organelle fragmentation and apoptosis induction was also observed using transient transfection of Bcl-2 without a GFP tag (data not shown). Furthermore, expression of GFP by itself did not cause any deleterious effects. The cell death caused by Bcl-2 expression was determined to be apoptotic since caspase-3 cleavage and DNA fragmentation were evident (Fig. 2). In addition, the caspase-3 inhibitor zVAD-FMK reduced the cell death evoked by Bcl-2 expression to close to control levels. Our data concur with previous studies that employed transient transfection of Bcl-2 and found increased levels of spontaneous apoptosis [4,29].

In our hands, stable expression of Bcl-2 provides a more suitable model for exploring Bcl-2 function. Transient and stable Bcl-2-expressing cells were initially transfected in the same manner. Thereafter, the transiently transfected cells were used ~16 h post-transfection, whilst the stable cells were allowed to grow in the presence of G418. It is likely that during the selection of stable Bcl-2-expressing transfectants, those cells with high levels of protein expression were eliminated by spontaneous apoptosis. The remaining population of cells had lower Bcl-2 expression and were protected from apoptosis. Moreover, the differences observed in the anti-apoptotic effects of low (i.e. low levels of BCl-2 expression achieved by transient or stable expression in TO-GFP-Bcl-2 expressing cells exhibited reduced organelle fragmentation compared to cells transiently expressing GFP-Bcl-2, but they were not as resistant to apoptotic stimuli as cells stably expressing GFP-Bcl-2) is suggestive that stable expression of Bcl-2 enhances the activity of other pro-survival pathways.

The precise mechanisms underlying the ability of high levels of Bcl-2 to cause organelle fragmentation and promote apoptosis are presently unclear. Our data suggest that excessive levels of Bcl-2 cause organelle fragmentation and cell death in a Ca^{2+}- and ROS-dependent manner (Figs. 7—9). Exactly how Bcl-2 leads to accumulation of Ca^{2+} and ROS is not known. It is established that Bcl-2 can be cleaved into a pro-apoptotic moiety by caspase-3, but mutation of the relevant amino acid (Asp 34) does not protect the cells from apoptosis [4]. It is possible that Bcl-2 may undergo additional forms of NH_2- or COOH-terminal processing when it is expressed at high levels [30]. Indeed, in our experiments with the greatest Bcl-2 expression levels, anti-Bcl-2 antibodies detected multiple bands in the immunoblots (e.g. Fig. 5A), consistent with proteolytic cleavage of the protein or accumulation of harmful truncated peptides. Further work is required to explore how and when Bcl-2 develops a pro-apoptotic configuration. However, it is interesting to note that cells possess an endogenous mechanism that limits the expression of Bcl-2. The 5′ and 3′ untranslated regions of human Bcl-2 mRNA contain sequences that negatively regulate transcription of Bcl-2 [31]. Expression of a Bcl-2 cDNA clones expressing the 5′ and 3′ untranslated regions reduces the cell death associated with Bcl-2 expression [30].

In summary, we see marked differences in the biological effect of Bcl-2 depending on its expression level. Other groups have also found concentration-dependent inverse effects of Bcl-2, for example on the activity of transcription factors [32]. These observations indicate that selection of the appropriate expression paradigm is crucial when trying to understand the biological role of Bcl-2. High levels of Bcl-2 cause apoptosis and severe organelle fragmentation. Either stable transfection or employing a regulated promoter appear to be the most appropriate methods to study Bcl-2 without inducing its pro-apoptotic action. In addition to its well-known role in promoting cell survival, Bcl-2 has a profound capacity to induce cell death via increases in cellular Ca^{2+} and ROS.

Acknowledgments

This work was supported by the BBSRC. CJH was the recipient of a BBSRC Ph.D. studentship. HLR is a Royal Society University Research Fellow.

References

[1] S. Cory, J.M. Adams, The Bcl2 family: regulators of the cellular life-or-death switch, Nat. Rev. Cancer 2 (2002) 647—656.
[2] Y. Tsujimoto, J. Yunis, L. Onorato-Showe, J. Erikson, P.C. Nowell, C.M. Croce, Molecular cloning of the chromosomal breakpoint of B-cell lymphomas and leukemias with the t(11;14) chromosome translocation, Science 224 (1984) 1403—1406.
[3] D.L. Vaux, S. Cory, J.M. Adams, Bcl-2 gene promotes haemopoietic cell survival and cooperates with c-myc to immortalize pre-B cells, Nature 335 (1988) 440—442.
[4] N.S. Wang, M.T. Unkila, E.Z. Reineks, C.W. Distelhorst, Transient expression of wild-type or mitochondrially targeted Bcl-2 induces apoptosis, whereas transient expression of endoplasmic reticulum-targeted Bcl-2 is protective against Bax-induced cell death, J. Biol. Chem. 276 (2001) 44117—44128.
[5] M.J. Berridge, P. Lipp, M.D. Bootman, The versatility and universality of calcium signalling, Nat. Rev. Mol. Cell. Biol. 1 (2000) 11—21.
[6] S. Gil-Parrado, A. Fernandez-Montalvan, I. Assfalg-Machleidt, O. Popp, F. Bestvater, A. Holloschi, T.A. Knoch, E.A. Auerswald, K. Welsh, J.C. Reed, H. Fritz, P. Fuentes-Prior, E. Spiess, G.S. Salvesen, W. Machleidt, Ionomycin-activated calpain triggers apoptosis. A probable role for Bcl-2 family members, J. Biol. Chem. 277 (2002) 27217—27226.
[7] I. Kruman, Q. Guo, M.P. Mattson, Calcium and reactive oxygen species mediate staurosporine-induced mitochondrial dysfunction and apoptosis in PC12 cells, J. Neurosci. Res. 51 (1998) 293—308.
[8] P. Pinton, R. Rizzuto, Bcl-2 and Ca2+ homeostasis in the endoplasmic reticulum, Cell. Death Differ. 13 (2006) 1409—1418.
[9] G. Szabadkai, R. Rizzuto, Participation of endoplasmic reticulum and mitochondrial calcium handling in apoptosis: more than just neighborhood? FEBS Lett. 567 (2004) 111—115.
[10] R. Chen, I. Valencia, F. Zhong, K.S. McColl, H.L. Roderick, M.D. Bootman, M.J. Berridge, S.J. Conway, A.B. Holmes, G.A. Mignery, P. Velez, C.W. Distelhorst, Bcl-2 functionally interacts with inositol 1,4,5-trisphosphate receptors to regulate calcium release from the ER in response to inositol 1,4,5-trisphosphate, J. Cell. Biol. 166 (2004) 193—203.
[11] M. Lam, G. Dubyak, L. Chen, G. Nunez, R.L. Miesfeld, C.W. Distelhorst, Evidence that BCL-2 represses apoptosis by regulating endoplasmic reticulum-associated Ca2+ fluxes, Proc. Natl. Acad. Sci. U.S.A. 91 (1994) 6569—6573.

[12] C. Li, C.J. Fox, S.R. Master, V.P. Bindokas, L.A. Chodosh, C.B. Thompson, Bcl-X(L) affects Ca(2+) homeostasis by altering expression of inositol 1,4,5-trisphosphate receptors, Proc. Natl. Acad. Sci. U.S.A. 99 (2002) 9830—9835.
[13] L. Scorrano, S.A. Oakes, J.T. Opferman, E.H. Cheng, M.D. Sorcinelli, T. Pozzan, S.J. Korsmeyer, BAX and BAK regulation of endoplasmic reticulum Ca2+: a control point for apoptosis, Science 300 (2003) 135—139.
[14] C.W. Distelhorst, G.C. Shore, Bcl-2 and calcium: controversy beneath the surface, Oncogene 23 (2004) 2875—2880.
[15] S.A. Oakes, L. Scorrano, J.T. Opferman, M.C. Bassik, M. Nishino, T. Pozzan, S.J. Korsmeyer, Proapoptotic BAX and BAK regulate the type 1 inositol trisphosphate receptor and calcium leak from the endoplasmic reticulum, Proc. Natl. Acad. Sci. U.S.A. 102 (2005) 105—110.
[16] T.H. Kuo, H.R. Kim, L. Zhu, Y. Yu, H.M. Lin, W. Tsang, Modulation of endoplasmic reticulum calcium pump by Bcl-2, Oncogene 17 (1998) 1903—1910.
[17] M.C. Bassik, L. Scorrano, S.A. Oakes, T. Pozzan, S.J. Korsmeyer, Phosphorylation of BCL-2 regulates ER Ca(2+) homeostasis and apoptosis, EMBO. J. 23 (2004) 1207—1216.
[18] L. Zhu, S. Ling, X.D. Yu, L.K. Venkatesh, T. Subramanian, G. Chinnadurai, T.H. Kuo, Modulation of mitochondrial Ca(2+) homeostasis by Bcl-2, J. Biol. Chem. 274 (1999) 33267—33273.
[19] F. Yao, T. Svensjo, T. Winkler, M. Lu, C. Eriksson, E. Eriksson, Tetracycline repressor, tetR, rather than the tetR-mammalian cell transcription factor fusion derivatives, regulates inducible gene expression in mammalian cells, Hum. Gene. Ther. 9 (1998) 1939—1950.
[20] H.L. Roderick, J.D. Lechleiter, P. Camacho, Cytosolic phosphorylation of calnexin controls intracellular Ca(2+) oscillations via an interaction with SERCA2b, J. Cell. Biol. 149 (2000) 1235—1248.
[21] C.M. Peppiatt, T.J. Collins, L. Mackenzie, S.J. Conway, A.B. Holmes, M.D. Bootman, M.J. Berridge, J.T. Seo, H.L. Roderick, 2-Aminoethoxydiphenyl borate (2-APB) antagonises inositol 1,4,5-trisphosphate-induced calcium release, inhibits calcium pumps and has a use-dependent and slowly reversible action on store-operated calcium entry channels, Cell Calcium 34 (2003) 97—108.
[22] C.A. Hetz, M. Hunn, P. Rojas, V. Torres, L. Leyton, A.F. Quest, Caspase-dependent initiation of apoptosis and necrosis by the Fas receptor in lymphoid cells: onset of necrosis is associated with delayed ceramide increase, J. Cell. Sci. 115 (2002) 4671—4683.
[23] K. Subramanian, T. Meyer, Calcium-induced restructuring of nuclear envelope and endoplasmic reticulum calcium stores, Cell 89 (1997) 963—971.
[24] C.M. Pedrosa Ribeiro, R.R. McKay, E. Hosoki, G.S. Bird, J.W. Putney Jr., Effects of elevated cytoplasmic calcium and protein kinase C on endoplasmic reticulum structure and function in HEK293 cells, Cell Calcium 27 (2000) 175—185.
[25] H.L. Roderick, T.J. Collins, M.J. Berridge, M.D. Bootman, Elevated cytosolic calcium leads to remodelling of mitochondria and the endoplasmic reticulum, J. Physiol. 547P (2003) PC33.
[26] I.I. Kruman, M.P. Mattson, Pivotal role of mitochondrial calcium uptake in neural cell apoptosis and necrosis, J. Neurochem. 72 (1999) 529—540.
[27] E. Petit, D. Divoux, Y. Chancerelle, J.F. Kergonou, A. Nouvelot, Immunological approach to investigating membrane cell damages induced by lipoperoxidative stress. Application to far UV-irradiated erythrocytes, Biol. Trace Elem. Res. 47 (1995) 17—27.
[28] C.J. Hanson, M.D. Bootman, H.L. Roderick, Cell signalling: IP3 receptors channel calcium into cell death, Curr. Biol. 14 (2004) R933—R935.
[29] N. Shinoura, Y. Yoshida, M. Nishimura, Y. Muramatsu, A. Asai, T. Kirino, H. Hamada, Expression level of Bcl-2 determines anti- or proapoptotic function, Cancer Res. 59 (1999) 4119—4128.
[30] T. Subramanian, G. Chinnadurai, Pro-apoptotic activity of transiently expressed BCL-2 occurs independent of BAX and BAK, J. Cell. Biochem. 89 (2003) 1102—1114.
[31] E.J. Uhlmann, T. Subramanian, C.A. Vater, R. Lutz, G. Chinnadurai, A potent cell death activity associated with transient high level expression of BCL-2, J. Biol. Chem. 273 (1998) 17926—17932.
[32] C.A. Massaad, B.P. Portier, G. Taglialatela, Inhibition of transcription factor activity by nuclear compartment-associated Bcl-2, J. Biol. Chem. 279 (2004) 54470—54478.